

VALIDATION OF A GEANT4 BASED MONTE CARLO CODE FOR VOXELIZED GEOMETRIES FOR PATIENT-ORIENTED MAMMOGRAPHY DOSIMETRY

Rahel-Debora Werner^{1*}, Marco A. Rodríguez-Jirón², Mariela A. Porras-Chaverri^{2,3}.

¹University of Halle-Wittenberg, Halle an der Saale, Germany

²School of Physics, University of Costa Rica, San José, Costa Rica.

³Atomic, Nuclear and Molecular Sciences Research Center, University of Costa Rica, San José, Costa Rica.

Received May 2021; accepted November 2021

Abstract

This work presents a preliminary validation of a Monte Carlo radiation transport code capable of simulating radiation transport on voxelized structures. Field size and depth dose were measured at Physikalisch-Technische Bundesanstalt (PTB) Braunschweig for mammography tungsten spectra of 30 kVp and 50kVp. Four different collimators were used to vary the field size between 0.94 cm and 4.74 cm of aperture radius. Depth dose was measured between 0 cm and 2 cm depth using a PTW PMMA phantom and two PTW ion chambers. Monte Carlo simulations were performed using the Geant4 toolkit (EM standard physics). Maximum relative difference in field size effect between experiment and simulation was 2.1%. In the case of the depth-dose study, it was 5.6%. The simulations used in this study have been shown to provide accurate estimations of quantities relevant to the calculation of dosimetric quantities.

Resumen

Este trabajo presenta una validación preliminar de un código Monte Carlo de transporte de radiación capaz de simular el transporte en estructuras. El tamaño del campo y la dosis de profundidad se midieron en Physikalisch-Technische Bundesanstalt (PTB) Braunschweig para espectros de tungsteno de mamografía de 30 kVp y 50kVp. Se utilizaron cuatro colimadores diferentes para variar el tamaño del campo entre 0,94 cm y 4,74 cm de radio de apertura. La dosis de profundidad se midió entre 0 cm y 2 cm de profundidad usando un maniquí de PMMA PTW y dos cámaras de iones PTW. Las simulaciones de Monte Carlo se realizaron utilizando el kit de herramientas Geant4 (física estándar EM). La diferencia relativa máxima en el efecto del tamaño del campo entre el experimento y la simulación fue del 2,1%. En el caso del estudio de dosis en profundidad, fue del 5,6%. Se ha demostrado que las simulaciones utilizadas en este estudio proporcionan estimaciones precisas de cantidades relevantes para el cálculo de dosis.

Keywords: Monte Carlo methods, experimental validation, radiation metrology

Palabras clave: métodos de Monte Carlo, validación experimental, metrología de radiaciones

I. INTRODUCTION

Computational medical physics is a vast field of study that has the potential to increase the output of scientific research in low- and middle-income countries, where access to funding for scientific equipment may be limited. In the case of Costa Rica, this field is emerging and has the potential to complement the technical training of medical physics graduate students. Practical training in computational resources used for medical physics applications, as well as developing their own methods as part of their thesis work, prepares future professionals with access to modern tools for clinical problem-solving.

However, one limitation of this field is the need to validate the methods used against experimental measurements. Often, this requires access to experimental equipment that is not available in low- and middle-income countries.

^{1*}Corresponding Author: rahel-debora@posteo.de

This work presents a preliminary validation of a Monte Carlo radiation transport code (Geant4, DICOM example by Archambault, Beaulieu and Hubert-Tremblay) capable of simulating radiation transport on voxelized structures using measurements of field size and depth dose. The experimental work for this initial study was made possible through a collaboration of one of the authors with *Physikalisch-Technische Bundesanstalt (PTB) Braunschweig* and was part of an undergraduate thesis developed at University of Halle-Wittenberg in Germany.

Moreover, this work provides an initial experimental basis for future scientific research in mammography dosimetry to be conducted at the Laboratorio de Física Médica Computacional (FIMEC, inaugurated in March 2019) at the Centro de Investigación en Ciencias Atómicas, Nucleares y Moleculares (Atomic, Nuclear and Molecular Sciences Research Center, CICANUM) at University of Costa Rica. Such research includes the further development of the heterogeneously-layered breast model (HLB) (Porras-Chaverri, 2014; 2012). This model has the potential to overcome the limitations of over the currently used models by Dance (1990) and Wu (1991), as it could avoid over- and underestimations of the personal mean glandular dose (MGD) as documented in Sarno et al. (2018). Additionally, it may find usage in quality assurance or epidemiological purposes. This Monte-Carlo code could be used to further advance this research at FIMEC but only after it has been against an experimental benchmark.

II. MATERIALS AND METHODS

The experimental validation of the MC-Code took place at PTB Braunschweig. The aim was to perform dose measurements in a mammography-like environment and simulate the irradiation under the same conditions for comparison between the experiment and simulation. Two separate experiments were conducted: one focusing on the field size effect and the other on the depth dose curve. All geometries described in the experimental setup were simulated using Geant4 (CERN, 2019), specifically the adapted DICOM example by Archambault, Beaulieu, and Hubert-Tremblay.

The laboratory setup for both experiments remained consistent and is depicted in Figure 1. To mimic mammary tissue, a "Soft X-Ray Slab Phantom" made of PMMA by PTW Freiburg was used. Dose measurements were carried out using two cylindrical "Soft X-Ray Ionization Chambers" of type 23342 and 23344 by PTW Freiburg, the specifications of which are provided in Table 1. In order to replicate beam qualities similar to those used in mammography, the experiments were conducted with two tungsten spectra: TW30 and TW50, as detailed in Table 2 and Figure 2.

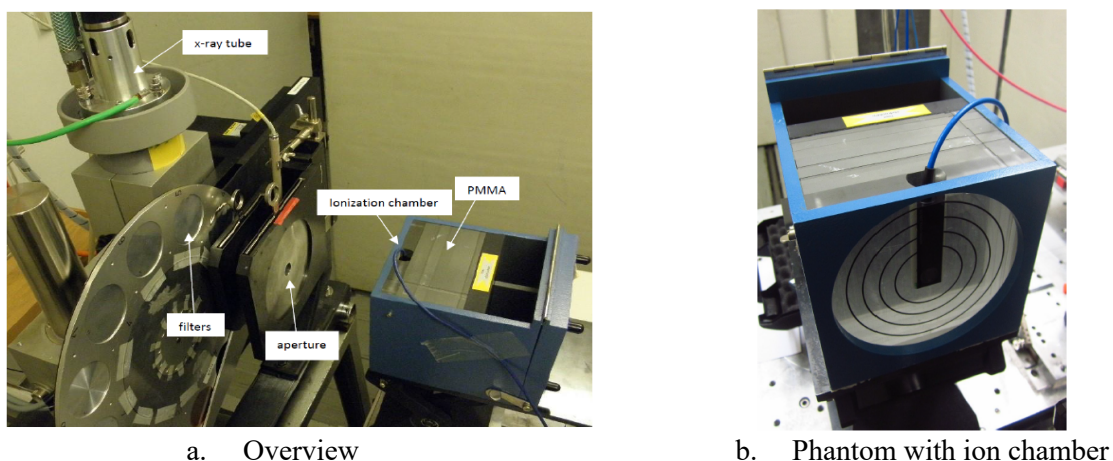


Figure 1. Laboratory settings for the measurements

Table 1. Characteristics of the ionization chambers 233342 and 23344 by PTW Freiburg

	IC 23343	IC 23342
Diameter	5.1 mm	15.9 mm
Depth	1.0 mm	1.5 mm
Sensitive volume	0.02 cm ³	0.3 cm ³

Table 2. Characteristics of tungsten spectra by PTB Braunschweig

DIN 6809-4	Tube voltage	Total filtration	1 st HVL	Mean energy (fluence)
TW30	30 kV	0.5 mm Al	0.359 mm Al	19.3 keV
TW50	50 kV	1.0 mm Al	0.940 mm Al	28.7 keV

To achieve different field sizes, the beam can be collimated using various lead diaphragms, resulting in approximate field sizes of 2 cm, 3 cm, 5 cm, and 10 cm. It is important to note that the focal spot of the x-ray tube is not point-like, which means that the intensity distribution is not a uniformly intense rectangle. Instead, it exhibits areas of penumbra at the edges and other field inhomogeneities, such as the Heel effect (Krieger, 2018, p. 124).

The effective field diameter can be calculated using the method described by Krauss et al. (2012, p. 6256). The widths of the penumbra (t) and the core field (c) can be measured or calculated using equation (1) with the following parameters: source-to-phantom distance (e), source-to-cover distance (a), cover aperture diameter (d), and focus size (f) (refer to Figure 3).

$$t = \frac{(d+f)e}{a} - f \text{ and } c = \frac{(d-f)}{a} + f \quad (1)$$

The effective field diameter d_{eff} is calculated with equation (2).

$$d_{eff} = \frac{c+t}{2} \quad (2)$$

The experiments in this work were performed with a distance $e = 293.5$ mm. The effective field sizes are listed in Table 3. The expected aberration between the calculated and measured field sizes is less than 1.5% and is included in the uncertainty (see Table 3). The field sizes used in the simulations were the same as those in the experiments, but unfortunately, the distance was set to a prior value of $e = 300$ mm. However, this difference is negligible as it only slightly affects the entry angle of the photons.

In the simulation, the radiation source G4GeneralParticleSource was utilized. It comprises a circular plane with a radius equal to the effective field size. This source emits homogeneous radiation and is positioned at a distance twice that of the phantom, directing its x-rays towards the location of the actual tube. Beyond the focus point, the rays diverge, forming a collimated cone and leading to a uniform intensity distribution in the irradiated region of the phantom.

For the field-size experiment, the objective was to study the impact of field size on the absorbed energy in the center of a radiation field. It is anticipated that the absorbed dose in the center of the field would increase with the size of the irradiated field due to back scattering and side scattering effects.

In the experiment, the ionization chambers (IC) were positioned at the center of the PMMA phantom. They were sequentially exposed to the TW30 and TW50 spectra, using the four different diaphragm sizes specified in Table 3. The uncertainties of the measured quantities or results are indicated in parentheses next to the respective values, representing the uncertainty of the last digit(s).

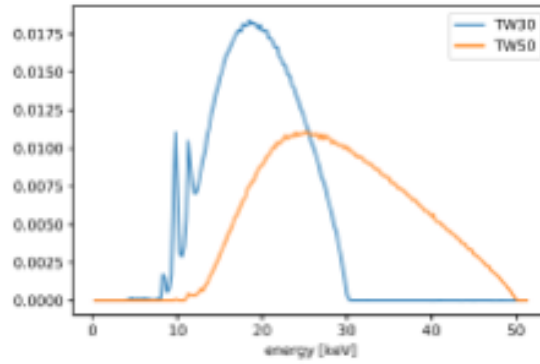


Figure 2. Normalized tungsten spectra used in the experiments.

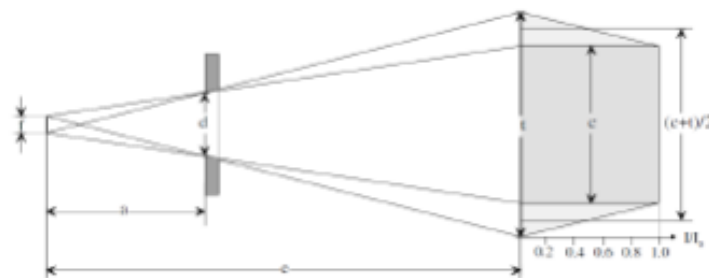


Figure 3. Schematic illustration of the path and intensity distribution of an x-ray beam emitted from a focus of finite size passing through an aperture. Caption and figure by Krauss et al (2012).

Table 3. Effective field sizes used in the experiments and simulations.

Diaphragm name	Effective field radius (cm)
D2	0.94 (3)
D3	1.42 (4)
D5	2.37 (6)
D10	4.74 (11)

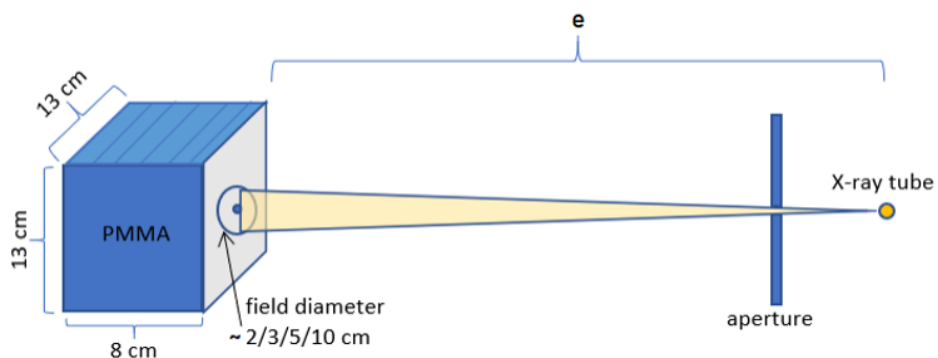


Figure 4. Simplified setting of the field size effect measurements

In the simulation, the cylindrical ionization chamber was replaced with a cuboid of the same volume. The cuboid has the same depth as the cylinder and two equal sides measuring 1.444 cm (for IC 23344) or 0.448 cm (for IC 23342). To increase the response, the chamber volume was filled with air at a density of 1 g/cm^3 , following the air composition specified by ICRU (1984). The simulations were performed using 109 particles. In the original DICOM example, the radiation source G4ParticleGun was used, which generates photons of a single energy. To simulate the spectra, G4ParticleGun was replaced with G4GeneralParticleSource, allowing for a user-defined spectrum represented as a histogram with 0.25 keV steps. In the simulation, there is a vacuum between the radiation source and the phantom to prevent additional attenuation or scattering, as the experimental spectrum was measured at the surface of the phantom.

In the depth-dose experiment, the depth dose curve in PMMA was measured and compared to simulations. Since breast tissue is comparable to PMMA (Dance, 1990, p. 12), similar depth dose curves can be expected for mammography. This experiment also demonstrates the importance of the location of glandular tissue in relation to the beam entrance. When glandular tissue is closer to the beam entrance and screened by skin and adipose tissue, it results in a lower mean glandular dose (MGD).

The experimental setup for this experiment is similar to the field size experiment. The position of the ionization chamber inside the phantom was varied by placing PMMA slabs of different thicknesses in front of the chamber. This allowed for the measurement of a depth dose curve using both TW30 and TW50 spectra with a constant field size (D3 aperture). To enhance the response, this experiment was conducted only with the IC 23344.

The simulations were performed using 108 photons on a similar geometry, with the cylindrical chamber replaced by a cuboid of the same volume, as described in the field size experiment. As an initial approximation, the chamber material was set to PMMA instead of air. This approximation was made based on the fact that the effective atomic number differs only by approximately 1. Simulating the chamber with PMMA increases the response and allows for the measurement of the complete depth dose curve within a single simulation, saving computational time.

III. RESULTS AND DISCUSSION

In the field-size effect experiment, the results were normalized to the largest field size, as shown in Figure 5. The experimental data points are accompanied by error bars in both the x and y directions. The uncertainty in the y direction encompasses all calibration and measurement uncertainties, including corrections for pressure, temperature, and the monitor chamber, among others. On the other hand, the error bar in the x direction represents the uncertainty in the effective field size, as indicated in Table 3. This uncertainty is not present in the simulated results.

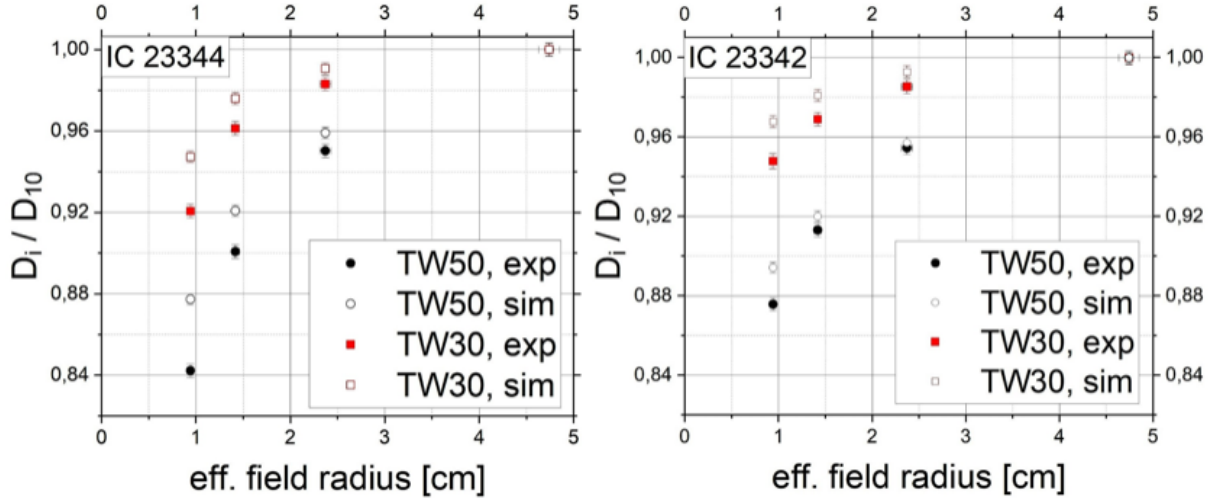


Figure 5. Results of the field size effect, doses normalized to largest field size (D10)

The vertical error bars in the simulation represent the standard deviation of three identical simulations using TW50. This spectrum is expected to have a higher statistical spread compared to TW30 due to its interactions with matter.

Both chamber curves exhibit a similar trend, where the dose decreases as the field size decreases. This behavior is expected since the drop in dose is primarily influenced by back scattering, which is approximately independent of chamber size.

However, there are differences observed in the relative difference R_i at a diaphragm i between the small and the large chamber, as calculated using equation (3).

$$R_i = \frac{\frac{D_{i,small}}{D_{10,small}} \frac{D_{i,large}}{D_{10,large}}}{\frac{D_{i,small}}{D_{10,small}}} \quad (3)$$

In the simulation, the relative differences R_5 and R_3 are both less than 0.6 % for both beam qualities. The relative difference R_2 is 2.1 % for TW30 and 1.9 % for TW50. In the experiment, the relative difference R_5 is less than 0.5 % for both spectra. R_3 is 0.8 % for TW30 and 1.4 % for TW50. R_2 is 2.9 % for TW30 and 3.8 % for TW50. The uncertainties associated with these values are on the order of the second decimal place, and therefore not shown.

The relative difference \tilde{R}_i between the experiment and simulation at a diaphragm i is calculated using equation (4).

$$\tilde{R}_i = \frac{D_{i,exp}}{D_{10,exp}} - \frac{\frac{D_{i,\sim}}{D_{10,\sim}}}{\frac{D_{i,exp}}{D_{10,exp}}} \quad (4)$$

This difference is attributed to the discrepancy caused by the rectangular voxel representing the sensitive volume in the simulation, as well as the bigger volume and field inhomogeneities of IC 23344 in the experiment.

By comparing the experimental and simulated results, it is observed that the IC 23344 data is excluded from the validation due to the larger reduction of scored dose caused by edge phenomena when decreasing the field size. Therefore, the focus of the first experiment is on the IC 23342.

The relative difference \tilde{R}_i is a measure of the deviation between the experiment and simulation, and it quantifies the agreement between the two.

The observed trend of the simulated data consistently being larger than the experimental data is maintained. \tilde{R}_5 is -0.268(2)% for TW50 and -0.766(3)% for TW30. \tilde{R}_3 is -0.755(3)% for TW50 and -1.242(5)% for TW30. \tilde{R}_2 is -2.105(10)% for TW30 and -2.107(9)% for TW50. It's important to note that the uncertainty in the x-direction, which is only present in the experimental data, is not considered in the uncertainty of \tilde{R}_i .

One possible reason for the discrepancy between the simulation and experiment is the difference in directional characteristics. In the simulation, the source has a flat intensity distribution at the irradiated area of the phantom, while the x-ray tube in the experiment exhibits an intensity maximum in the center of the field. This difference can lead to a larger proportion of photons traveling at larger angles in the simulation compared to the experiment, resulting in higher absorbed doses in the simulation.

Another factor that may contribute to the deviation is the difference in chamber properties. In the simulation, the cylindrical volume of the chamber was replaced with a cuboid of the same volume, and the air filling the sensitive volume was replaced with air of higher density. Other materials of the chamber, such as the polyethylene entrance window and graphite electrodes, were not included in the simulation. These differences in chamber composition may affect the response and contribute to the observed discrepancies.

The choice of the physics list used in the simulation should also be considered. It has been suggested that using physics lists such as G4EmLivermorePhysics or G4EmStandardPhysics-Option4 could result in better agreement between simulation and experiment, especially for low-energy physics. However, this was not explored in the current study.

It is worth noting that other published validations of Geant4-based Monte Carlo codes have reported relative differences between experiment and simulation of up to 9%. Furthermore, the determination of mean glandular dose (MGD) using current methods is only possible within an uncertainty of approximately 13%. Therefore, a maximum relative difference of -2.107(9)% is deemed acceptable, and the usage of this Monte Carlo code for MGD estimates is justified.

The depth dose curve for the two spectra, normalized to the first depth, is shown in Figure 6 (left). The vertical error bars for the experimental data are calculated using the same method as in the field size experiment. The horizontal error bars represent the uncertainty in slab thickness, which is not present in the simulation. The uncertainty caused by the field size was assessed by simulating the depth dose experiment while varying the field size within the bounds specified by its uncertainty (Table 3). The resulting changes are of the same order of magnitude as the statistical uncertainty, both being less than 0.5%. The combined effect of these uncertainties is reflected in the vertical error bars.

Indeed, the choice of the physics list in the simulation is an important consideration. According to Fedon (2015), G4EmStandardPhysics may not be the most suitable choice for accurately describing low-energy physics. It is expected that using physics lists like G4EmLivermorePhysics or G4EmStandardPhysics-Option4 would lead to better agreement between simulation and experiment (Fedon, 2015). Although this was not explored in the current thesis, it is recognized as a priority for future work.

It is worth noting that other published validations of Geant4-based Monte Carlo codes have reported relative differences between experiment and simulation of up to 9% (Carrier, 2004, p. 488) (Fedon, 2015, p. 316). Additionally, the determination of mean glandular dose (MGD) using current methods is only possible within an uncertainty of approximately 13%. Therefore, the maximum relative difference of -2.107(9)% observed in this study is considered acceptable, and the usage of this Monte Carlo code for MGD estimates is justified.

The depth dose curve for the two spectra, normalized to the first depth, is displayed in Figure 6 (left). The vertical error bars for the experimental data are calculated using the same method as in the field size experiment. The horizontal error bars represent the uncertainty in slab thickness, which is not accounted for in the simulation. The uncertainty resulting from the variation in field size was assessed by conducting

simulations of the depth dose experiment while varying the field size within the limits specified by its uncertainty (Table 3). The resulting changes are of the same order of magnitude as the statistical uncertainty, both being less than 0.5%. The combination of these uncertainties constitutes the vertical error bar in the plot.

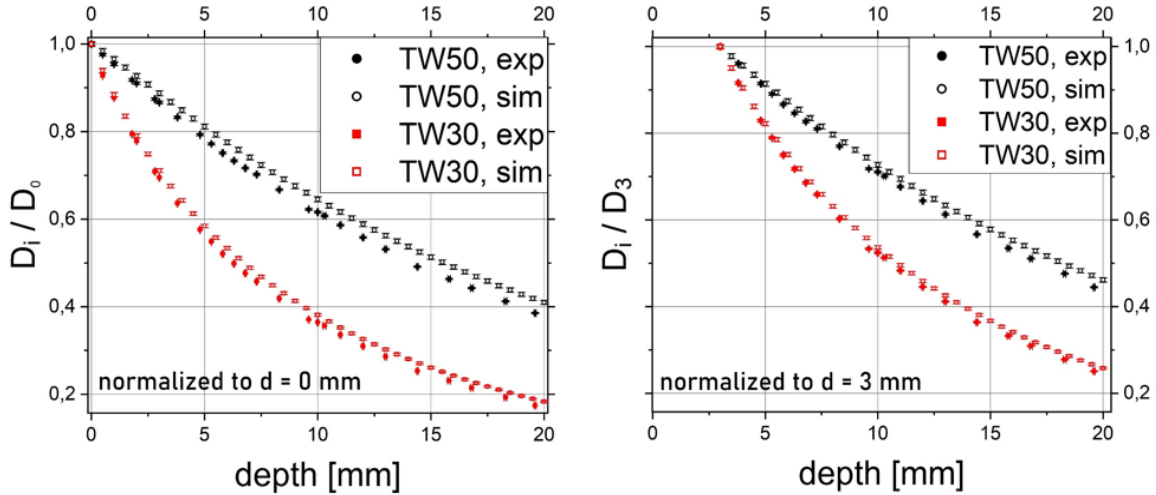


Figure 6. Depth dose curve in a PMMA slab phantom (experiment versus simulation). Left: doses normalized to a depth of 0 mm. Right: doses normalized to a depth of 3 mm.

The depth dose curve for TW30 exhibits a faster decrease compared to TW50, which can be attributed to the larger mass attenuation coefficient of TW30. When shielded by 2 cm of PMMA, the dose decreases to approximately 20% and 40% of the maximum dose for TW30 and TW50, respectively.

The comparison between the experimental and simulated depth dose curves reveals that the experimental curve shows a faster decrease than the simulated curve. This difference is more pronounced for TW50 compared to TW30. One source of error is the field inhomogeneity experienced by IC 23344, as investigated in the field size experiment. To mitigate this effect, the curves were normalized to a depth of 3 mm, where the field is more homogeneous (Figure 6, right).

Upon normalizing the doses to a different depth, omitting the initial few points, the curves converge. This supports the assumption that a field property is the primary difference between the simulation and experiment. Consequently, the subsequent comparison between simulation and experiment is focused on the curve normalized to 3 mm.

The simulated doses were measured at intervals of 0.5 mm, while the experimental values were only available at uneven depths depending on the available slab thicknesses. Data points for the same depths were only available at 1, 2, 3, 10, 11, 12, and 13 mm. The data for other depths were determined through linear interpolation.

From a depth of 3 mm to 19.5 mm, the dose decreases by 74.7(3)% in the experiment and by 73.3(3)% in the simulation for the lower-energy spectrum. For TW50, the dose decreases by 55.3(4)% in the experiment and by 52.8(5)% in the simulation.

The relative difference $R(d)$ at a depth d between the experiment and simulation is calculated using equation (5).

$$R(d) = \frac{\frac{D_{\text{exp}}(d)}{D_{\text{exp}}(0)} - \frac{D(d)}{D(0)}}{\frac{D_{\text{exp}}(d)}{D_{\text{exp}}(0)}} \quad (5)$$

The relative difference R increases with larger depths and reaches a maximum of 5.60(5)% for TW50 and 5.53(5)% for TW30 at a depth of 19.5 mm. The average relative difference for all depths between 3 mm and 19.5 mm with steps of 0.5 mm is 2.9(15)% for both qualities.

To improve this experiment, using IC 23342 could be considered as it would be less affected by field inhomogeneities. Alternatively, using the next cover size (D5) could enhance the field homogeneity over the detector. Nonlinear interpolation could also be explored to further minimize the relative difference R .

The simulation can be enhanced by using a different Geant4 PhysicsList, as discussed in the field size experiment. Other sources of discrepancy, such as the source and chamber characteristics, are also addressed there.

Considering a maximum relative difference of 5.60(5)% between simulation and experiment, this validates the code with the same justification as before.

IV. CONCLUSIONS

This work presents the successful experimental validation of a Geant4-based MC code for patient-oriented mammography dosimetry. The validation included two experiments conducted at PTB Braunschweig, using two different low-energy spectra.

In the field size experiment, the simulation reproduced the field size effect with a maximum relative difference of -2.107(9)% compared to the experiment. This indicates a good agreement between the simulated and experimental data.

In the depth dose experiment, the simulation of the depth dose curve in PMMA showed an average relative difference of 2.9(15)% to the experimental data for both spectra. The maximum relative difference was 5.60(5)%. While there are some discrepancies between the simulation and experiment, it is important to note that the uncertainty associated with the calculation of the mean glandular dose (MGD) is much larger than these differences. Additionally, comparisons with other published studies have shown similar or larger differences between experiments and simulations.

Based on these results, it can be concluded that the initial experimental validation of this MC code for mammography dosimetry is successful. However, there is room for improvement, such as exploring different Geant4 PhysicsLists and considering other sources of discrepancy. Further studies and refinements can be undertaken to enhance the accuracy and reliability of the MC code for practical applications in mammography dosimetry.

V. REFERENCES

- Carrier F. J., Archambault, L., Beaulieu, L. & Roy, R. (2004) Validation of GEANT4, an object-oriented Monte Carlo toolkit, for simulations in medical physics. *Medical Physics* 31(3) pp. 484–492.
- CERN. (2019) *Geant4 - A simulation toolkit*. url: <http://geant4.web.cern.ch/> (visited on 08/21/2019).
- Dance, D.R. (1990) Monte carlo calculation of conversion factors for the estimation of mean glandular breast dose. *Physics in Medicine and Biology* 35(9), pp. 1211–1219.
- Fedon, C., Longo, F., Mettivier, G. & Longo, R. (2015) GEANT4 for breast dosimetry: parameters optimization study. *Physics in Medicine and Biology* 60, pp. 311–232.
- ICRU. *ICRU Report 37: Stopping Powers for Electrons and Positrons*. Tech. rep. 1984, p. 27.
- Krauss, A., Büermann, L., Kramer, H-M., Selbach, H-J. (2012) Calorimetric determination of the absorbed dose to water for medium-energy X-rays with generating voltages from 70 to 280 kV". *Physics in Medicine and Biology* 57, p. 6256.
- Krieger, H. (2018) *Strahlungsquellen für Technik und Medizin*. Springer Spektrum, 2018

- Porras-Chaverri, M.A. (2014) *Patient-oriented breast imaging dosimetry for conventional mammography*. (Doctoral thesis) University of Wisconsin-Madison, Madison, Wisconsin, United States of America.
- Porras-Chaverri, M. A., Mora, P., Vetter, J.R., Highnam, R. (2016) Determination of Personalized Mean Glandular Dose Using Estimates of Glandular Tissue Distribution in a Clinical Setting”. *Asociación Latinoamericana de Física Médica* 2(1) pp. 69–72.
- Porras-Chaverri, M. A., Vetter, J.R., Highnam, R. (2012) Personalizing mammographic dosimetry using multilayered anatomy-based breast models. Breast Imaging. IWDM 2012. *Lecture Notes in Computer Science*, 7361 pp. 134-140.
- Sarno A., Mettivier, G., Di Lillo, F., Bliznakova, K., Sechopoulos, I, Russo, P. (2018) Homogeneous vs. patient specific breast models for Monte Carlo evaluation of mean glandular dose in mammography. *Physica Medica* 51, pp. 56–63.
- Wi, X., Barnes, G.T., and Tucker, D.M. (1991) Spectral Dependence of Glandular Tissue Dose in Screen-Film Mammography. *Radiology* 179, pp. 143–148.

ACKNOWLEDGMENTS

The authors wish to acknowledge the valuable contributions of the Working Group 6.25 at PTB Braunschweig: Steffen Ketelhut, Ina Warkehr, Ludwig Büermann, Reinulf Böttcher, Ulrike Ankerhold and Ralf-Peter Kapsch, as well as Youming Yang and Eric Simiele.